Advances in Quantitative MRI: Acquisition, Estimation, and Applications

Gopal Nataraj

Dissertation Proposal
May 15, 2017

Dept. of Electrical Engineering and Computer Science
University of Michigan

Goal: rapidly and reliably localize biomarkers from MR data

Goal: rapidly and reliably localize biomarkers from MR data

- biomarker   measurable tissue property (*e.g.*, elasticity) that
              characterizes a biological process (*e.g.*, sclerosis)

Goal: rapidly and reliably localize biomarkers from MR data

- biomarker   measurable tissue property (*e.g.*, elasticity) that characterizes a biological process (*e.g.*, sclerosis)
- localize   produce quantitative MR images

Goal: rapidly and reliably localize biomarkers from MR data

- biomarker   measurable tissue property (*e.g.*, elasticity) that
              characterizes a biological process (*e.g.*, sclerosis)
- localize   produce quantitative MR images
- rapidly   fast acquisition, fast estimation

Goal: rapidly and reliably localize biomarkers from MR data

- biomarker   measurable tissue property (*e.g.*, elasticity) that characterizes a biological process (*e.g.*, sclerosis)
- localize   produce quantitative MR images
- rapidly   fast acquisition, fast estimation
- reliably   accurate signal models, precise estimation

Goal: rapidly and reliably localize biomarkers from MR data

- biomarker   measurable tissue property (*e.g.*, elasticity) that characterizes a biological process (*e.g.*, sclerosis)
- localize   produce quantitative MR images
- rapidly   fast acquisition, fast estimation
- reliably   accurate signal models, precise estimation

Challenges (beyond conventional MRI):

- complicated, nonlinear signal models
- more data required, so longer scan times

Advances in Quantitative MRI:

- **Acquisition** [Ch. 4]

  How can we assemble fast, informative collections of scans
  to enable precise biomarker quantification?

Advances in Quantitative MRI:

- **Acquisition** [Ch. 4]
  How can we assemble fast, informative collections of scans
  to enable precise biomarker quantification?

- **Estimation** [Ch. 5]
  Given data from an informative acquisition,
  how can we rapidly and accurately quantify these biomarkers?

Advances in Quantitative MRI:

- **Acquisition**   [Ch. 4]
  How can we assemble fast, informative collections of scans
  to enable precise biomarker quantification?

- **Estimation**   [Ch. 5]
  Given data from an informative acquisition,
  how can we rapidly and accurately quantify these biomarkers?

- **Application**   [Ch. 6]
  Using these tools, can we design a state-of-the-art biomarker?

Advances in Quantitative MRI:

- **Acquisition**   [Ch. 4]

  How can we assemble fast, informative collections of scans
  to enable precise biomarker quantification?

- **Estimation**   [Ch. 5]

  Given data from an informative acquisition,
  how can we rapidly and accurately quantify these biomarkers?

- **Application**   [Ch. 6]

  Using these tools, can we design a state-of-the-art biomarker?

Signal Model

After reconstruction, single voxel y_d in dth image modeled as

$$y_d = s_d(\mathbf{x}; \boldsymbol{\nu}, \mathbf{p}_d) + \epsilon_d \tag{1}$$

- $\mathbf{x} \in \mathbb{R}^L$ latent free parameters
- $\boldsymbol{\nu} \in \mathbb{R}^K$ known parameters
- $\mathbf{p}_d \in \mathbb{R}^A$ acquisition parameters
- $s_d : \mathbb{R}^{L+K+A} \mapsto \mathbb{C}$ dth signal model
- $\epsilon_d \in \mathbb{C}$ noise $\sim \mathbb{CN}(0, \sigma_d^2)$

Signal Model

A *scan profile* contains D voxels $\mathbf{y} := [y_1, \ldots, y_D]^\mathsf{T}$, modeled as

$$\mathbf{y} = \mathbf{s}(\mathbf{x}; \boldsymbol{\nu}, \mathbf{P}) + \boldsymbol{\epsilon} \qquad (1)$$

- $\mathbf{x} \in \mathbb{R}^L$ latent free parameters
- $\boldsymbol{\nu} \in \mathbb{R}^K$ known parameters
- $\mathbf{P} := [\mathbf{p}_1, \ldots, \mathbf{p}_D]$ acquisition parameter matrix
- $\mathbf{s} : \mathbb{R}^{L+K+AD} \mapsto \mathbb{C}^D$ vector signal model
- $\boldsymbol{\epsilon} \sim \mathbb{C}\mathcal{N}(\mathbf{0}_D, \boldsymbol{\Sigma})$ noise, with $\boldsymbol{\Sigma} := \mathrm{diag}\big(\sigma_1^2, \ldots, \sigma_D^2\big)$

Signal Model

A *scan profile* contains D voxels $\mathbf{y} := [y_1, \ldots, y_D]^\mathsf{T}$, modeled as

$$\mathbf{y} = \mathbf{s}(\mathbf{x}; \boldsymbol{\nu}, \mathbf{P}) + \boldsymbol{\epsilon} \tag{1}$$

- $\mathbf{x} \in \mathbb{R}^L$ latent free parameters
- $\boldsymbol{\nu} \in \mathbb{R}^K$ known parameters
- $\mathbf{P} := [\mathbf{p}_1, \ldots, \mathbf{p}_D]$ acquisition parameter matrix
- $\mathbf{s} : \mathbb{R}^{L+K+AD} \mapsto \mathbb{C}^D$ vector signal model
- $\boldsymbol{\epsilon} \sim \mathbb{CN}(\mathbf{0}_D, \boldsymbol{\Sigma})$ noise, with $\boldsymbol{\Sigma} := \mathrm{diag}\big(\sigma_1^2, \ldots, \sigma_D^2\big)$

Task: design $\mathbf{P}$ to enable precise unbiased estimation of $\mathbf{x}$

When $\mathbf{s}$ is analytic in $\mathbf{x}$ (as is typical),

Fisher information characterizes unbiased estimator precision:

$$\mathbf{F}(\mathbf{x}; \boldsymbol{\nu}, \mathbf{P}) := (\nabla_{\mathbf{x}}\mathbf{s}(\mathbf{x}; \boldsymbol{\nu}, \mathbf{P}))^{\mathsf{H}} \boldsymbol{\Sigma}^{-1} \nabla_{\mathbf{x}}\mathbf{s}(\mathbf{x}; \boldsymbol{\nu}, \mathbf{P}). \qquad (2)$$

When $\mathbf{s}$ is analytic in $\mathbf{x}$ (as is typical),
Fisher information characterizes unbiased estimator precision:

$$\mathbf{F}(\mathbf{x}; \boldsymbol{\nu}, \mathbf{P}) := (\nabla_{\mathbf{x}} \mathbf{s}(\mathbf{x}; \boldsymbol{\nu}, \mathbf{P}))^{\mathsf{H}} \Sigma^{-1} \nabla_{\mathbf{x}} \mathbf{s}(\mathbf{x}; \boldsymbol{\nu}, \mathbf{P}). \qquad (2)$$

When $\mathbf{F}$ is invertible, Cramér-Rao Bound (CRB) [Cramér, 1946]
ensures covariance of unbiased estimates $\widehat{\mathbf{x}}$ of $\mathbf{x}$ satisfy

$$\mathrm{cov}(\widehat{\mathbf{x}}; \boldsymbol{\nu}, \mathbf{P}) \succeq \mathbf{F}^{-1}(\mathbf{x}; \boldsymbol{\nu}, \mathbf{P}). \qquad (3)$$

When $\mathbf{s}$ is analytic in $\mathbf{x}$ (as is typical),
Fisher information characterizes unbiased estimator precision:

$$\mathbf{F}(\mathbf{x}; \boldsymbol{\nu}, \mathbf{P}) := (\nabla_{\mathbf{x}}\mathbf{s}(\mathbf{x}; \boldsymbol{\nu}, \mathbf{P}))^{\mathsf{H}}\Sigma^{-1}\nabla_{\mathbf{x}}\mathbf{s}(\mathbf{x}; \boldsymbol{\nu}, \mathbf{P}). \qquad (2)$$

When $\mathbf{F}$ is invertible, Cramér-Rao Bound (CRB) [Cramér, 1946]
ensures covariance of unbiased estimates $\widehat{\mathbf{x}}$ of $\mathbf{x}$ satisfy

$$\mathrm{cov}(\widehat{\mathbf{x}}; \boldsymbol{\nu}, \mathbf{P}) \succeq \mathbf{F}^{-1}(\mathbf{x}; \boldsymbol{\nu}, \mathbf{P}). \qquad (3)$$

Maximum-likelihood (ML) estimates achieve CRB asymptotically
or equivalently (for Gaussian data) at sufficiently high SNR.

When **s** is analytic in **x** (as is typical),
Fisher information characterizes unbiased estimator precision:

$$\mathbf{F}(\mathbf{x}; \boldsymbol{\nu}, \mathbf{P}) := (\nabla_{\mathbf{x}}\mathbf{s}(\mathbf{x}; \boldsymbol{\nu}, \mathbf{P}))^{\mathsf{H}} \Sigma^{-1} \nabla_{\mathbf{x}}\mathbf{s}(\mathbf{x}; \boldsymbol{\nu}, \mathbf{P}). \quad (2)$$

When **F** is invertible, Cramér-Rao Bound (CRB)   [Cramér, 1946]
ensures covariance of unbiased estimates $\widehat{\mathbf{x}}$ of **x** satisfy

$$\mathrm{cov}(\widehat{\mathbf{x}}; \boldsymbol{\nu}, \mathbf{P}) \succeq \mathbf{F}^{-1}(\mathbf{x}; \boldsymbol{\nu}, \mathbf{P}). \quad (3)$$

Maximum-likelihood (ML) estimates achieve CRB asymptotically
or equivalently (for Gaussian data) at sufficiently high SNR.
Idea: choose **P** such that imprecision matrix $\mathbf{F}^{-1}$ "small"

Scan Design

Idea: choose $\mathbf{P}$ to minimize the objective

$$\Psi(\mathbf{x}; \boldsymbol{\nu}, \mathbf{P}) = \text{tr}\left(\mathbf{W}\mathbf{F}^{-1}(\mathbf{x}; \boldsymbol{\nu}, \mathbf{P})\mathbf{W}^{\mathsf{T}}\right), \tag{4}$$

where $\mathbf{W} \in \mathbb{R}^{L \times L}$ is a pre-selected diagonal matrix of weights.

Idea: choose $\mathbf{P}$ to minimize the objective

$$\Psi(\mathbf{x}; \boldsymbol{\nu}, \mathbf{P}) = \text{tr}\left(\mathbf{W}\mathbf{F}^{-1}(\mathbf{x}; \boldsymbol{\nu}, \mathbf{P})\mathbf{W}^{\mathsf{T}}\right), \qquad (4)$$

where $\mathbf{W} \in \mathbb{R}^{L \times L}$ is a pre-selected diagonal matrix of weights.

Challenge: $\mathbf{x}, \boldsymbol{\nu}$ vary spatially

Scan Design

Idea: choose $\mathbf{P}$ to minimize the objective

$$\Psi(\mathbf{x}; \boldsymbol{\nu}, \mathbf{P}) = \text{tr}\left(\mathbf{W}\mathbf{F}^{-1}(\mathbf{x}; \boldsymbol{\nu}, \mathbf{P})\mathbf{W}^{\mathsf{T}}\right), \tag{4}$$

where $\mathbf{W} \in \mathbb{R}^{L \times L}$ is a pre-selected diagonal matrix of weights.

Challenge: $\mathbf{x}, \boldsymbol{\nu}$ vary spatially

Two problems considered:

- min-max scan design   [Nataraj et al., 2017]

$$\check{\mathbf{P}} \in \left\{ \arg \min_{\mathbf{P} \in \mathbb{P}} \max_{\substack{\mathbf{x} \in \mathbb{X}^{\mathrm{t}} \\ \boldsymbol{\nu} \in \mathbb{N}^{\mathrm{t}}}} \Psi(\mathbf{x}; \boldsymbol{\nu}, \mathbf{P}), \right\} \tag{5}$$

where $\mathbb{X}^{\mathrm{t}} \subseteq \mathbb{R}^{L}$ and $\mathbb{N}^{\mathrm{t}} \subseteq \mathbb{R}^{K}$ are "tight" ranges of interest and $\mathbb{P}$ is defined by acquisition/timing constraints

Scan Design

Idea: choose $\mathbf{P}$ to minimize the objective

$$\Psi(\mathbf{x}; \boldsymbol{\nu}, \mathbf{P}) = \text{tr}\Big(\mathbf{W}\mathbf{F}^{-1}(\mathbf{x}; \boldsymbol{\nu}, \mathbf{P})\mathbf{W}^\mathsf{T}\Big), \tag{4}$$

where $\mathbf{W} \in \mathbb{R}^{L \times L}$ is a pre-selected diagonal matrix of weights.

Challenge: $\mathbf{x}, \boldsymbol{\nu}$ vary spatially

Two problems considered:

- min-max scan design [Nataraj et al., 2017]

$$\check{\mathbf{P}} \in \left\{ \arg\min_{\mathbf{P} \in \mathbb{P}} \max_{\substack{\mathbf{x} \in \mathbb{X}^t \\ \boldsymbol{\nu} \in \mathbb{N}^t}} \Psi(\mathbf{x}; \boldsymbol{\nu}, \mathbf{P}), \right\} \tag{5}$$

- Bayesian scan design [§6.3]

$$\check{\mathbf{P}} \in \left\{ \arg\min_{\mathbf{P} \in \mathbb{P}} \mathsf{E}_{\mathbf{x}, \boldsymbol{\nu}}(\Psi(\mathbf{x}; \boldsymbol{\nu}, \mathbf{P})) \right\} \tag{6}$$

Scan Design

Idea: choose $\mathbf{P}$ to minimize the objective

$$\Psi(\mathbf{x}; \nu, \mathbf{P}) = \text{tr}\left(\mathbf{W}\mathbf{F}^{-1}(\mathbf{x}; \nu, \mathbf{P})\mathbf{W}^{\top}\right), \tag{4}$$

where $\mathbf{W} \in \mathbb{R}^{L \times L}$ is a pre-selected diagonal matrix of weights.

Challenge: $\mathbf{x}, \nu$ vary spatially

Two problems considered:

- min-max scan design   [Nataraj et al., 2017]

$$\check{\mathbf{P}} \in \left\{ \arg \min_{\mathbf{P} \in \mathbb{P}} \max_{\substack{\mathbf{x} \in \mathbb{X}^{\text{t}} \\ \nu \in \mathbb{N}^{\text{t}}}} \Psi(\mathbf{x}; \nu, \mathbf{P}), \right\} \tag{5}$$

- Bayesian scan design   [§6.3]

$$\check{\mathbf{P}} \in \left\{ \arg \min_{\mathbf{P} \in \mathbb{P}} \mathsf{E}_{\mathbf{x}, \nu}(\Psi(\mathbf{x}; \nu, \mathbf{P})) \right\} \tag{6}$$

Task: design fast acquisition for precise estimation of relaxation parameters T_1, T_2 in white/gray matter (WM/GM) of brain

Task: design fast acquisition for precise estimation of relaxation parameters T_1, T_2 in white/gray matter (WM/GM) of brain

- Consider scan profiles consisting of two fast pulse sequences
  - Spoiled Gradient-Recalled Echo (SPGR)   [Zur et al., 1991]
  - Dual-Echo Steady-State (DESS)   [Redpath and Jones, 1988]

Detailed Example Study

Task: design fast acquisition for precise estimation of relaxation parameters T_1, T_2 in white/gray matter (WM/GM) of brain

- Consider scan profiles consisting of two fast pulse sequences
  - Spoiled Gradient-Recalled Echo (SPGR)   [Zur et al., 1991]
  - Dual-Echo Steady-State (DESS)   [Redpath and Jones, 1988]
- For each scan profile feasible under total time constraint:
  1. Let **s** model corresponding single-component signal
     - $\mathbf{x} \leftarrow [m_0, T_1, T_2]^\mathsf{T}$, where m_0 is a scale factor
     - $\boldsymbol{\nu} \leftarrow$ flip angle variation
     - $\mathbf{P} \leftarrow$ nominal flip angles, repetition times
  2. Optimize **P** subject to flip angle, sequence timing constraints
     - $\mathbf{W} \leftarrow \mathrm{diag}(0, 0.1, 1)$ emphasizes T_1, T_2 est roughly equally
     - $\mathbb{X}^\mathrm{t}$ chosen to focus on WM/GM at 3T field strength
     - $\mathbb{N}^\mathrm{t}$ chosen to allow 10% flip angle variation

(#SPGR, #DESS) Profiles	$(2, 1)$	$(1, 1)$	$(0, 2)$
SPGR nom. flip (deg)	(15, 5)	15	–
DESS nom. flip (deg)	30	10	(35, 10)
SPGR rep. times (ms)	(12.2, 12.2)	13.9	–
DESS rep. times (ms)	17.5	28.0	(24.4, 17.5)
Optimized Cost	4.0	4.9	**3.5**

(#SPGR, #DESS) Profiles	$(2,1)$	$(1,1)$	$(0,2)$
SPGR nom. flip (deg)	(15, 5)	15	–
DESS nom. flip (deg)	30	10	(35, 10)
SPGR rep. times (ms)	(12.2, 12.2)	13.9	–
DESS rep. times (ms)	17.5	28.0	(24.4, 17.5)
Optimized Cost	4.0	4.9	**3.5**

Main finding: 2 DESS sequences can yield T_1, T_2 WM/GM estimates that are at least as precise as T_1, T_2 estimates from SPGR/DESS scan profiles, under this competitive time constraint.

- Simulated many WM-like, GM-like voxel realizations
- Studied sample statistics of T_1, T_2 ML estimates $\widehat{T}_1^{\mathrm{ML}}$, $\widehat{T}_2^{\mathrm{ML}}$

Numerical Simulation

- Simulated many WM-like, GM-like voxel realizations
- Studied sample statistics of T_1, T_2 ML estimates $\widehat{T}_1^{\mathrm{ML}}$, $\widehat{T}_2^{\mathrm{ML}}$

Profile	$(2,1)$	$(1,1)$	$(0,2)$	Truth
WM $\widehat{T}_1^{\mathrm{ML}}$	830 ± 17	830 ± 15	830 ± 14	832
GM $\widehat{T}_1^{\mathrm{ML}}$	$1330 \pm 30.$	1330 ± 24	1330 ± 24	1331
WM $\widehat{T}_2^{\mathrm{ML}}$	$80. \pm 1.0$	$80. \pm 2.1$	79.6 ± 0.94	79.6
GM $\widehat{T}_2^{\mathrm{ML}}$	$110. \pm 1.4$	$110. \pm 3.0$	$110. \pm 1.6$	110

Table 1: $\widehat{T}_1^{\mathrm{ML}}$, $\widehat{T}_2^{\mathrm{ML}}$ sample means $\pm$ sample standard deviations

Experimental Setup

Candidate $(2,1)$, $(1,1)$, $(0,2)$ SPGR/DESS scan profiles

- Prescribed optimized nominal flip angles, repetition times
- Used $256 \times 256 \times 8$ 3D matrix over $24 \times 24 \times 4$cm FOV
- Required **1m37s** scan time for each profile

Experimental Setup

Candidate $(2, 1)$, $(1, 1)$, $(0, 2)$ SPGR/DESS scan profiles

- Prescribed optimized nominal flip angles, repetition times
- Used $256 \times 256 \times 8$ 3D matrix over $24 \times 24 \times 4$cm FOV
- Required **1m37s** scan time for each profile

Reference scan profile

- Four inversion recovery (IR) scans for T_1 estimation
- Four spin-echo (SE) scans for T_2 estimation
- 256×256 matrix over $24 \times 24 \times 0.5$cm FOV
- Required **40m58s** scan time total

Experimental Setup

Candidate $(2,1)$, $(1,1)$, $(0,2)$ SPGR/DESS scan profiles

- Prescribed optimized nominal flip angles, repetition times
- Used $256 \times 256 \times 8$ 3D matrix over $24 \times 24 \times 4$cm FOV
- Required **1m37s** scan time for each profile

Reference scan profile

- Four inversion recovery (IR) scans for T_1 estimation
- Four spin-echo (SE) scans for T_2 estimation
- 256×256 matrix over $24 \times 24 \times 0.5$cm FOV
- Required **40m58s** scan time total

Bloch-Siegert (BS) acquisition for separate flip angle calibration

- Acquired 2 BS-shifted SPGR scans in 1m40s total

(a) $\widehat{T}_1^{\mathrm{ML}}$ Estimates

(b) $\widehat{T}_2^{\mathrm{ML}}$ Estimates

Compared against NIST NMR measurements [Keenan et al., 2016]

- Repeated each profile 10 times
- Estimated T_1, T_2 std dev of typical voxel across repetitions

Phantom Precision Results

	(2, 1)	(1, 1)	(0, 2)
V5 $\widehat{\sigma}_{\widehat{T}_1^{\mathrm{ML}}}$	50 ± 12	$40 \pm 10.$	39 ± 9.4
V6 $\widehat{\sigma}_{\widehat{T}_1^{\mathrm{ML}}}$	70 ± 18	60 ± 15	70 ± 16
V7 $\widehat{\sigma}_{\widehat{T}_1^{\mathrm{ML}}}$	60 ± 13	50 ± 13	50 ± 13
V5 $\widehat{\sigma}_{\widehat{T}_2^{\mathrm{ML}}}$	2.6 ± 0.63	6 ± 1.4	3.5 ± 0.84
V6 $\widehat{\sigma}_{\widehat{T}_2^{\mathrm{ML}}}$	1.9 ± 0.46	5 ± 1.1	2.3 ± 0.54
V7 $\widehat{\sigma}_{\widehat{T}_2^{\mathrm{ML}}}$	1.4 ± 0.34	3.4 ± 0.80	1.5 ± 0.35

Table 2: Pooled sample standard deviations $\pm$ pooled standard errors of sample standard deviations (ms), from optimized SPGR/DESS profiles.

Phantom Precision Results

	(2, 1)	(1, 1)	(0, 2)
V5 $\widehat{\sigma}_{\widehat{T}_1^{\mathrm{ML}}}$	50 ± 12	$40 \pm 10.$	39 ± 9.4
V6 $\widehat{\sigma}_{\widehat{T}_1^{\mathrm{ML}}}$	70 ± 18	60 ± 15	70 ± 16
V7 $\widehat{\sigma}_{\widehat{T}_1^{\mathrm{ML}}}$	60 ± 13	50 ± 13	50 ± 13
V5 $\widehat{\sigma}_{\widehat{T}_2^{\mathrm{ML}}}$	2.6 ± 0.63	6 ± 1.4	3.5 ± 0.84
V6 $\widehat{\sigma}_{\widehat{T}_2^{\mathrm{ML}}}$	1.9 ± 0.46	5 ± 1.1	2.3 ± 0.54
V7 $\widehat{\sigma}_{\widehat{T}_2^{\mathrm{ML}}}$	1.4 ± 0.34	3.4 ± 0.80	1.5 ± 0.35

Table 2: Pooled sample standard deviations $\pm$ pooled standard errors of sample standard deviations (ms), from optimized SPGR/DESS profiles.

Similar trends across profiles of empirical vs. theoretical std dev!

../fig/c,scn-dsgn/2016-05-31,brain,t1-ml,jet.eps

../fig/c,scn-dsgn/2016-05-31,brain,t2-ml,jet.eps

Figure 1: Colorbar ranges in ms.

Contributions

- MR scan design method for precise parameter estimation
- Fast SPGR/DESS scan profile for T_1, T_2 estimation in brain

Contributions

- MR scan design method for precise parameter estimation
- Fast SPGR/DESS scan profile for T_1, T_2 estimation in brain
  - Simulation and phantom results validate method
    as a predictor of unbiased estimation precision.

Contributions

- MR scan design method for precise parameter estimation
- Fast SPGR/DESS scan profile for T_1, T_2 estimation in brain
  - Simulation and phantom results validate method
    as a predictor of unbiased estimation precision.
  - *In vivo* results reveal discrepancies (especially in T_2 estimates),
    suggesting sensitivity to model mismatch.

Summary

Contributions

- MR scan design method for precise parameter estimation
- Fast SPGR/DESS scan profile for T_1, T_2 estimation in brain
  - Simulation and phantom results validate method
    as a predictor of unbiased estimation precision.
  - *In vivo* results reveal discrepancies (especially in T_2 estimates),
    suggesting sensitivity to model mismatch.

How to address model mismatch?

- More complete *in vivo* signal models
- More scalable parameter estimation

Advances in Quantitative MRI:

- **Acquisition**   [Ch. 4]
  How can we assemble fast, informative collections of scans
  to enable precise biomarker quantification?

- **Estimation**   [Ch. 5]
  Given data from an informative acquisition,
  how can we rapidly and accurately quantify these biomarkers?

- **Application**   [Ch. 6]
  Using these tools, can we design a state-of-the-art biomarker?

Given: at each voxel, image sequence $\mathbf{y} \in \mathbb{C}^D$ modeled as

$$\mathbf{y} = \mathbf{s}(\mathbf{x}, \boldsymbol{\nu}) + \boldsymbol{\epsilon} \tag{7}$$

- $\mathbf{x} \in \mathbb{R}^L$ latent free parameters
- $\boldsymbol{\nu} \in \mathbb{R}^K$ known parameters
- $\mathbf{s} : \mathbb{R}^{L+K} \mapsto \mathbb{C}^D$ vector signal model
- $\boldsymbol{\epsilon} \in \mathbb{C}^D$ noise $\sim \mathbb{C}\mathcal{N}(\mathbf{0}_D, \boldsymbol{\Sigma})$

Signal Model

Given: at each voxel, image sequence $\mathbf{y} \in \mathbb{C}^D$ modeled as

$$\mathbf{y} = \mathbf{s}(\mathbf{x}, \boldsymbol{\nu}) + \boldsymbol{\epsilon} \tag{7}$$

- $\mathbf{x} \in \mathbb{R}^L$ latent free parameters
- $\boldsymbol{\nu} \in \mathbb{R}^K$ known parameters
- $\mathbf{s} : \mathbb{R}^{L+K} \mapsto \mathbb{C}^D$ vector signal model
- $\boldsymbol{\epsilon} \in \mathbb{C}^D$ noise $\sim \mathbb{CN}(\mathbf{0}_D, \boldsymbol{\Sigma})$

Task: construct fast estimator $\widehat{\mathbf{x}}(\mathbf{y}, \boldsymbol{\nu})$

Task: construct fast estimator $\widehat{\mathbf{x}}(\mathbf{y}, \boldsymbol{\nu})$

Challenges:

- signal $\mathbf{s}$ often nonlinear in $\mathbf{x}$: non-convex inverse problems
- signal $\mathbf{s}$ might be difficult to write in closed form

Task: construct fast estimator $\widehat{\mathbf{x}}(\mathbf{y}, \boldsymbol{\nu})$

Challenges:

- signal **s** often nonlinear in **x**: non-convex inverse problems
- signal **s** might be difficult to write in closed form

Conventional Approaches:

- gradient-based local optimization
    - initialization-dependent solution
    - requires signal gradients

Prior Work

Task: construct fast estimator $\widehat{\mathbf{x}}(\mathbf{y}, \boldsymbol{\nu})$

Challenges:

- signal **s** often nonlinear in **x**: non-convex inverse problems
- signal **s** might be difficult to write in closed form

Conventional Approaches:

- gradient-based local optimization
  - initialization-dependent solution
  - requires signal gradients
- stochastic methods (*e.g.*, simulated annealing)
  - unclear convergence analysis   [Bertsimas and Tsitsiklis, 1993]
  - several unintuitive tuning parameters

Prior Work

Task: construct fast estimator $\widehat{\mathbf{x}}(\mathbf{y}, \boldsymbol{\nu})$

Challenges:

- signal **s** often nonlinear in **x**: non-convex inverse problems
- signal **s** might be difficult to write in closed form

Conventional Approaches:

- gradient-based local optimization
  - initialization-dependent solution
  - requires signal gradients
- stochastic methods (*e.g.*, simulated annealing)
  - unclear convergence analysis   [Bertsimas and Tsitsiklis, 1993]
  - several unintuitive tuning parameters
- grid search   *e.g.*, for 1-compartment relaxivity [Ch. 4]

Grid search computational costs

	L	$\sim$number dictionary atoms
1-compartment relaxivity	3	$\sim 100^2$

Grid search computational costs

	L	$\sim$number dictionary atoms
1-compartment relaxivity	3	$\sim 100^2$
flow velocity	4	$\sim 100^3$
diffusivity tensor	7	$\sim 100^6$
2-3 compartment relaxivity	6-10	$\sim 100^5 - 100^9$

Grid search computational costs

	L	$\sim$number dictionary atoms
1-compartment relaxivity	3	$\sim 100^2$
flow velocity	4	$\sim 100^3$
diffusivity tensor	7	$\sim 100^6$
2-3 compartment relaxivity	6-10	$\sim 100^5 - 100^9$

Can we scale computation with L more gracefully?

Idea: learn a *nonlinear* estimator from simulated training data

Idea: learn a *nonlinear* estimator from simulated training data

- sample $(\mathbf{x}_1, \boldsymbol{\nu}_1, \epsilon_1), \ldots, (\mathbf{x}_N, \boldsymbol{\nu}_N, \epsilon_N)$ from prior distributions
- simulate image data vectors $\mathbf{y}_1, \ldots, \mathbf{y}_N$ via signal model $\mathbf{s}$

Machine Learning for QMRI Parameter Estimation

Idea: learn a *nonlinear* estimator from simulated training data

- sample $(\mathbf{x}_1, \boldsymbol{\nu}_1, \epsilon_1), \ldots, (\mathbf{x}_N, \boldsymbol{\nu}_N, \epsilon_N)$ from prior distributions
- simulate image data vectors $\mathbf{y}_1, \ldots, \mathbf{y}_N$ via signal model $\mathbf{s}$
- design *nonlinear* functions $\widehat{x}_l(\cdot) := \widehat{h}_l(\cdot) + \widehat{b}_l$ for $l \in \{1, \ldots, L\}$ that map each $\mathbf{q}_n := [\mathrm{Re}(\mathbf{y}_n)^{\mathsf{T}}, \mathrm{Im}(\mathbf{y}_n)^{\mathsf{T}}, \boldsymbol{\nu}_n^{\mathsf{T}}]^{\mathsf{T}} \in \mathcal{Q}$ to $x_{l,n} \in \mathbb{R}$

Machine Learning for QMRI Parameter Estimation

Idea: learn a *nonlinear* estimator from simulated training data

- sample $(\mathbf{x}_1, \boldsymbol{\nu}_1, \epsilon_1), \ldots, (\mathbf{x}_N, \boldsymbol{\nu}_N, \epsilon_N)$ from prior distributions
- simulate image data vectors $\mathbf{y}_1, \ldots, \mathbf{y}_N$ via signal model $\mathbf{s}$
- design *nonlinear* functions $\widehat{x}_l(\cdot) := \widehat{h}_l(\cdot) + \widehat{b}_l$ for $l \in \{1, \ldots, L\}$ that map each $\mathbf{q}_n := [\mathrm{Re}(\mathbf{y}_n)^{\mathsf{T}}, \mathrm{Im}(\mathbf{y}_n)^{\mathsf{T}}, \boldsymbol{\nu}_n^{\mathsf{T}}]^{\mathsf{T}} \in \mathcal{Q}$ to $x_{l,n} \in \mathbb{R}$

$$\left(\widehat{h}_l, \widehat{b}_l\right) \in \left\{ \arg \min_{\substack{h_l \\ b_l \in \mathbb{R}}} \frac{1}{N} \sum_{n=1}^{N} (h_l(\mathbf{q}_n) + b_l - x_{l,n})^2 \right\}$$

Idea: learn a *nonlinear* estimator from simulated training data

- sample $(\mathbf{x}_1, \boldsymbol{\nu}_1, \epsilon_1), \ldots, (\mathbf{x}_N, \boldsymbol{\nu}_N, \epsilon_N)$ from prior distributions
- simulate image data vectors $\mathbf{y}_1, \ldots, \mathbf{y}_N$ via signal model $\mathbf{s}$
- design *nonlinear* functions $\widehat{x}_l(\cdot) := \widehat{h}_l(\cdot) + \widehat{b}_l$ for $l \in \{1, \ldots, L\}$ that map each $\mathbf{q}_n := [\mathrm{Re}(\mathbf{y}_n)^\mathsf{T}, \mathrm{Im}(\mathbf{y}_n)^\mathsf{T}, \boldsymbol{\nu}_n^\mathsf{T}]^\mathsf{T} \in \mathcal{Q}$ to $x_{l,n} \in \mathbb{R}$

$$\left(\widehat{h}_l, \widehat{b}_l \right) \in \left\{ \arg \min_{\substack{h_l \\ b_l \in \mathbb{R}}} \frac{1}{N} \sum_{n=1}^{N} (h_l(\mathbf{q}_n) + b_l - x_{l,n})^2 \right\} \quad \text{ill-posed!}$$

Machine Learning for QMRI Parameter Estimation

Idea: learn a *nonlinear* estimator from simulated training data

- sample $(\mathbf{x}_1, \nu_1, \epsilon_1), \ldots, (\mathbf{x}_N, \nu_N, \epsilon_N)$ from prior distributions
- simulate image data vectors $\mathbf{y}_1, \ldots, \mathbf{y}_N$ via signal model $\mathbf{s}$
- design *nonlinear* functions $\widehat{x}_l(\cdot) := \widehat{h}_l(\cdot) + \widehat{b}_l$ for $l \in \{1, \ldots, L\}$
  that map each $\mathbf{q}_n := [\mathrm{Re}(\mathbf{y}_n)^\mathsf{T}, \mathrm{Im}(\mathbf{y}_n)^\mathsf{T}, \boldsymbol{\nu}_n^\mathsf{T}]^\mathsf{T} \in \mathcal{Q}$ to $x_{l,n} \in \mathbb{R}$

$$\left(\widehat{h}_l, \widehat{b}_l \right) \in \left\{ \arg \min_{\substack{h_l \in \mathbb{H} \\ b_l \in \mathbb{R}}} \frac{1}{N} \sum_{n=1}^{N} (h_l(\mathbf{q}_n) + b_l - x_{l,n})^2 + \rho_l \|h_l\|_{\mathbb{H}}^2 \right\} \quad (8)$$

Solution: solve a *kernel ridge regression* (KRR) problem

- restrict function space over which we optimize
- include function regularization

Hilbert space: complete inner product function space

Hilbert space: complete inner product function space

Reproducing kernel Hilbert space (RKHS)

Hilbert space $\mathbb{H}$ over input space $\mathcal{Q}$ with *reproducing property*

$$\langle h, k(\cdot, \mathbf{q})\rangle_{\mathbb{H}} = h(\mathbf{q}), \qquad \forall h \in \mathbb{H}, \mathbf{q} \in \mathcal{Q}$$

for some $k : \mathcal{Q}^2 \mapsto \mathbb{R}$ called a reproducing kernel (RK)

Hilbert space: complete inner product function space

Reproducing kernel Hilbert space (RKHS)

Hilbert space $\mathbb{H}$ over input space $\mathcal{Q}$ with *reproducing property*

$$\langle h, k(\cdot, \mathbf{q})\rangle_{\mathbb{H}} = h(\mathbf{q}), \qquad \forall h \in \mathbb{H}, \mathbf{q} \in \mathcal{Q}$$

for some $k : \mathcal{Q}^2 \mapsto \mathbb{R}$ called a reproducing kernel (RK)

Relevant facts

- Bijection between RKHS $\mathbb{H}$ and RK k [Aronszajn, 1950]
- Function $k(\cdot, \mathbf{q}) \in \mathbb{H}$ called a *feature mapping*

Choose: RK $k : \mathcal{Q}^2 \mapsto \mathbb{R}$, which induces choice of RKHS $\mathbb{H}$

Choose: RK $k : \mathcal{Q}^2 \mapsto \mathbb{R}$, which induces choice of RKHS $\mathbb{H}$

- *Nonlinear* kernel corresponds to *nonlinear* estimation
- We use $k(\mathbf{q}, \mathbf{q}') \leftarrow \exp\left(-\frac{1}{2}\left\|\mathbf{\Lambda}^{-1}(\mathbf{q} - \mathbf{q}')\right\|_2^2\right)$

Choose: RK $k : \mathcal{Q}^2 \mapsto \mathbb{R}$, which induces choice of RKHS $\mathbb{H}$

Solve: for each desired latent parameter $l \in \{1, \ldots, L\}$,

$$\left(\widehat{h}_l, \widehat{b}_l\right) \in \left\{ \arg \min_{\substack{h_l \in \mathbb{H} \\ b_l \in \mathbb{R}}} \frac{1}{N} \sum_{n=1}^{N} (h_l(\mathbf{q}_n) + b_l - x_{l,n})^2 + \rho_l \|h_l\|_{\mathbb{H}}^2 \right\} \quad (9)$$

Function Optimization over a RKHS

Choose: RK $k : \mathcal{Q}^2 \mapsto \mathbb{R}$, which induces choice of RKHS $\mathbb{H}$

Solve: for each desired latent parameter $l \in \{1, \ldots, L\}$,

$$\left(\widehat{h}_l, \widehat{b}_l \right) \in \left\{ \arg \min_{\substack{h_l \in \mathbb{H} \\ b_l \in \mathbb{R}}} \frac{1}{N} \sum_{n=1}^{N} (h_l(\mathbf{q}_n) + b_l - x_{l,n})^2 + \rho_l \|h_l\|_{\mathbb{H}}^2 \right\} \quad (9)$$

- Optimal $\widehat{h}_l$ over $\mathbb{H}$ takes form   [Schölkopf et al., 2001]

$$\widehat{h}_l(\cdot) \equiv \sum_{n=1}^{N} \widehat{a}_{l,n} k(\cdot, \mathbf{q}_n) \quad (10)$$

Function Optimization over a RKHS

Choose: RK $k : \mathcal{Q}^2 \mapsto \mathbb{R}$, which induces choice of RKHS $\mathbb{H}$

Solve: for each desired latent parameter $l \in \{1, \ldots, L\}$,

$$\left(\widehat{h}_l, \widehat{b}_l\right) \in \left\{ \arg\min_{\substack{h_l \in \mathbb{H} \\ b_l \in \mathbb{R}}} \frac{1}{N} \sum_{n=1}^{N} (h_l(\mathbf{q}_n) + b_l - x_{l,n})^2 + \rho_l \|h_l\|_{\mathbb{H}}^2 \right\} \quad (9)$$

- Optimal $\widehat{h}_l$ over $\mathbb{H}$ takes form   [Schölkopf et al., 2001]

$$\widehat{h}_l(\cdot) \equiv \sum_{n=1}^{N} \widehat{a}_{l,n} k(\cdot, \mathbf{q}_n) \quad (10)$$

- Plug (10) into (9); solve now instead for $\left(\widehat{a}_l, \widehat{b}_l\right)$; construct:

$$\widehat{x}_l(\cdot) = \sum_{n=1}^{N} \widehat{a}_{l,n} k(\cdot, \mathbf{q}_n) + \widehat{b}_l \quad (11)$$

Non-iterative closed-form solution, for $l \in \{1, \dots, L\}$:

$$\widehat{x}_l(\cdot) = \mathbf{x}_l^\mathsf{T} \left(\frac{1}{N}\mathbf{1}_N + \mathbf{M}(\mathbf{KM} + N\rho_l\mathbf{I}_N)^{-1}\left(\mathbf{k}(\cdot) - \frac{1}{N}\mathbf{K}\mathbf{1}_N \right) \right) \quad (12)$$

- $\mathbf{x}_l := [x_{l,1}, \dots, x_{l,N}]^\mathsf{T}$ training pt regressands

Non-iterative closed-form solution, for $l \in \{1, \ldots, L\}$:

$$\widehat{x}_l(\cdot) = \mathbf{x}_l^\mathsf{T} \left(\frac{1}{N} \mathbf{1}_N + \mathbf{M}(\mathbf{KM} + N\rho_l \mathbf{I}_N)^{-1} \left(\mathbf{k}(\cdot) - \frac{1}{N} \mathbf{K} \mathbf{1}_N \right) \right) \quad (12)$$

- $\mathbf{x}_l := [x_{l,1}, \ldots, x_{l,N}]^\mathsf{T}$ training pt regressands

- $\mathbf{K} := \begin{bmatrix} k(\mathbf{q}_1, \mathbf{q}_1) & \cdots & k(\mathbf{q}_1, \mathbf{q}_N) \\ \vdots & \ddots & \vdots \\ k(\mathbf{q}_N, \mathbf{q}_1) & \cdots & k(\mathbf{q}_N, \mathbf{q}_N) \end{bmatrix}$ Gram matrix

MRI Parameter Estimation via KRR

Non-iterative closed-form solution, for $l \in \{1, \ldots, L\}$:

$$\widehat{x}_l(\cdot) = \mathbf{x}_l^\top \left(\frac{1}{N} \mathbf{1}_N + \mathbf{M}(\mathbf{K}\mathbf{M} + N\rho_l \mathbf{I}_N)^{-1} \left(\mathbf{k}(\cdot) - \frac{1}{N} \mathbf{K}\mathbf{1}_N \right) \right) \quad (12)$$

- $\mathbf{x}_l := [x_{l,1}, \ldots, x_{l,N}]^\top$ training pt regressands

- $\mathbf{K} := \begin{bmatrix} k(\mathbf{q}_1, \mathbf{q}_1) & \cdots & k(\mathbf{q}_1, \mathbf{q}_N) \\ \vdots & \ddots & \vdots \\ k(\mathbf{q}_N, \mathbf{q}_1) & \cdots & k(\mathbf{q}_N, \mathbf{q}_N) \end{bmatrix}$ Gram matrix

- $\mathbf{M} := \mathbf{I}_N - \frac{1}{N} \mathbf{1}_N \mathbf{1}_N^\top$ de-meaning operator

MRI Parameter Estimation via KRR

Non-iterative closed-form solution, for $l \in \{1, \ldots, L\}$:

$$\widehat{x}_l(\cdot) = \mathbf{x}_l^\mathsf{T} \left(\frac{1}{N}\mathbf{1}_N + \mathbf{M}(\mathbf{KM} + N\rho_l\mathbf{I}_N)^{-1}\left(\mathbf{k}(\cdot) - \frac{1}{N}\mathbf{K}\mathbf{1}_N \right) \right) \quad (12)$$

- $\mathbf{x}_l := [x_{l,1}, \ldots, x_{l,N}]^\mathsf{T}$ training pt regressands

- $\mathbf{K} := \begin{bmatrix} k(\mathbf{q}_1, \mathbf{q}_1) & \cdots & k(\mathbf{q}_1, \mathbf{q}_N) \\ \vdots & \ddots & \vdots \\ k(\mathbf{q}_N, \mathbf{q}_1) & \cdots & k(\mathbf{q}_N, \mathbf{q}_N) \end{bmatrix}$ Gram matrix

- $\mathbf{M} := \mathbf{I}_N - \frac{1}{N}\mathbf{1}_N\mathbf{1}_N^\mathsf{T}$ de-meaning operator

- $\mathbf{k}(\cdot) := [k(\cdot, \mathbf{q}_1), \ldots, k(\cdot, \mathbf{q}_N)]^\mathsf{T}$ nonlin kernel embedding

Non-iterative closed-form solution, for $l \in \{1, \ldots, L\}$:

$$\widehat{x}_l(\cdot) = \mathbf{x}_l^\mathsf{T} \left(\frac{1}{N} \mathbf{1}_N + \mathbf{M}(\mathbf{KM} + N\rho_l \mathbf{I}_N)^{-1} \left(\mathbf{k}(\cdot) - \frac{1}{N} \mathbf{K} \mathbf{1}_N \right) \right) \quad (12)$$

- $\mathbf{x}_l := [x_{l,1}, \ldots, x_{l,N}]^\mathsf{T}$ training pt regressands

- $\mathbf{K} := \begin{bmatrix} k(\mathbf{q}_1, \mathbf{q}_1) & \cdots & k(\mathbf{q}_1, \mathbf{q}_N) \\ \vdots & \ddots & \vdots \\ k(\mathbf{q}_N, \mathbf{q}_1) & \cdots & k(\mathbf{q}_N, \mathbf{q}_N) \end{bmatrix}$ Gram matrix

- $\mathbf{M} := \mathbf{I}_N - \frac{1}{N} \mathbf{1}_N \mathbf{1}_N^\mathsf{T}$ de-meaning operator

- $\mathbf{k}(\cdot) := [k(\cdot, \mathbf{q}_1), \ldots, k(\cdot, \mathbf{q}_N)]^\mathsf{T}$ nonlin kernel embedding

Can we scale computation with L more gracefully?

- Yes, in fact (12) separable in $l \in \{1, \ldots, L\}$ by construction

MRI Parameter Estimation via KRR

Non-iterative closed-form solution, for $l \in \{1, \ldots, L\}$:

$$\widehat{x}_l(\cdot) = \mathbf{x}_l^\mathsf{T} \left(\frac{1}{N} \mathbf{1}_N + \mathbf{M}(\mathbf{KM} + N\rho_l \mathbf{I}_N)^{-1} \left(\mathbf{k}(\cdot) - \frac{1}{N} \mathbf{K} \mathbf{1}_N \right) \right) \quad (12)$$

- $\mathbf{x}_l := [x_{l,1}, \ldots, x_{l,N}]^\mathsf{T}$ training pt regressands

- $\mathbf{K} := \begin{bmatrix} k(\mathbf{q}_1, \mathbf{q}_1) & \cdots & k(\mathbf{q}_1, \mathbf{q}_N) \\ \vdots & \ddots & \vdots \\ k(\mathbf{q}_N, \mathbf{q}_1) & \cdots & k(\mathbf{q}_N, \mathbf{q}_N) \end{bmatrix}$ Gram matrix

- $\mathbf{M} := \mathbf{I}_N - \frac{1}{N} \mathbf{1}_N \mathbf{1}_N^\mathsf{T}$ de-meaning operator

- $\mathbf{k}(\cdot) := [k(\cdot, \mathbf{q}_1), \ldots, k(\cdot, \mathbf{q}_N)]^\mathsf{T}$ nonlin kernel embedding

Can we scale computation with L more gracefully?

- Yes, in fact (12) separable in $l \in \{1, \ldots, L\}$ by construction

Suppose there exists "approximate feature mapping" $\tilde{\mathbf{z}} : \mathcal{Q} \mapsto \mathbb{R}^Z$ such that $\tilde{\mathbf{Z}} := [\tilde{\mathbf{z}}(\mathbf{q}_1), \ldots, \tilde{\mathbf{z}}(\mathbf{q}_N)]$ has for $\dim(\mathcal{Q}) \ll Z \ll N$

$$\mathbf{K} \approx \tilde{\mathbf{Z}}^\mathsf{T} \tilde{\mathbf{Z}}. \tag{13}$$

KRR as High-Dimensional Affine Regression

Suppose there exists "approximate feature mapping" $\tilde{\mathbf{z}} : \mathcal{Q} \mapsto \mathbb{R}^Z$ such that $\tilde{\mathbf{Z}} := [\tilde{\mathbf{z}}(\mathbf{q}_1), \dots, \tilde{\mathbf{z}}(\mathbf{q}_N)]$ has for $\dim(\mathcal{Q}) \ll Z \ll N$

$$\mathbf{K} \approx \tilde{\mathbf{Z}}^\mathsf{T}\tilde{\mathbf{Z}}. \tag{13}$$

Plugging (13) into KRR solution (12) and rearranging gives

$$\widehat{x}_l(\cdot) \approx \frac{1}{N}\mathbf{x}_l^\mathsf{T}\mathbf{1}_N + \frac{1}{N}\mathbf{x}_l^\mathsf{T}\mathbf{M}\tilde{\mathbf{Z}}^\mathsf{T}\left(\frac{1}{N}\tilde{\mathbf{Z}}\mathbf{M}\tilde{\mathbf{Z}}^\mathsf{T} + \rho_l\mathbf{I}_Z\right)^{-1}\left(\tilde{\mathbf{z}}(\cdot) - \frac{1}{N}\tilde{\mathbf{Z}}\mathbf{1}_N\right)$$

Suppose there exists "approximate feature mapping" $\tilde{\mathbf{z}} : \mathcal{Q} \mapsto \mathbb{R}^Z$ such that $\tilde{\mathbf{Z}} := [\tilde{\mathbf{z}}(\mathbf{q}_1), \ldots, \tilde{\mathbf{z}}(\mathbf{q}_N)]$ has for $\dim(\mathcal{Q}) \ll Z \ll N$

$$\mathbf{K} \approx \tilde{\mathbf{Z}}^\mathsf{T} \tilde{\mathbf{Z}}. \tag{13}$$

Plugging (13) into KRR solution (12) and rearranging gives

$$\widehat{x}_l(\cdot) \approx \widehat{m}_{x_l} + \widehat{\mathbf{c}}_{x_l \tilde{\mathbf{z}}}^\mathsf{T} \left(\widehat{\mathbf{C}}_{\tilde{\mathbf{z}}\tilde{\mathbf{z}}} + \rho_l \mathbf{I}_Z \right)^{-1} (\tilde{\mathbf{z}}(\cdot) - \widehat{\mathbf{m}}_{\tilde{\mathbf{z}}}) \tag{14}$$

which is regularized ("ridge") Z-dimensional affine regression!

KRR as High-Dimensional Affine Regression

Suppose there exists "approximate feature mapping" $\tilde{z} : \mathcal{Q} \mapsto \mathbb{R}^Z$ such that $\tilde{Z} := [\tilde{z}(q_1), \ldots, \tilde{z}(q_N)]$ has for $\dim(\mathcal{Q}) \ll Z \ll N$

$$K \approx \tilde{Z}^\mathsf{T} \tilde{Z}. \tag{13}$$

Plugging (13) into KRR solution (12) and rearranging gives

$$\widehat{x}_l(\cdot) \approx \widehat{m}_{x_l} + \widehat{c}_{x_l \tilde{z}}^\mathsf{T} \left(\widehat{C}_{\tilde{z}\tilde{z}} + \rho_l I_Z \right)^{-1} (\tilde{z}(\cdot) - \widehat{m}_{\tilde{z}}) \tag{14}$$

which is regularized ("ridge") Z-dimensional affine regression!

Does such a $\tilde{z}$ exist and work well in practice?

- Yes, *e.g.* for "shift invariant" kernels (like our Gaussian) of form $k(q, q') \equiv k(q - q')$ [Rahimi and Recht, 2007]
- In such cases, can reduce from $\sim N^2$ to $\sim NZ$ computations

Online model selection: train *after* observing (unlabeled) test data

Model Selection

Online model selection: train *after* observing (unlabeled) test data

- Prior on known ν density estimation
- Noise covariance Σ low-signal data regions

Model Selection

Online model selection: train *after* observing (unlabeled) test data

- Prior on known ν density estimation
- Noise covariance Σ low-signal data regions
- Regularization parameters   Bayesian perspective...

Online model selection: train *after* observing (unlabeled) test data

- Prior on known ν density estimation
- Noise covariance Σ low-signal data regions
- Regularization parameters   Bayesian perspective...

  - Assume prior $h_l(\cdot) + b_l \sim \mathcal{GP}(0(\cdot), k(\cdot, \cdot)), l \in \{1, \ldots, L\}$

Online model selection: train *after* observing (unlabeled) test data

- Prior on known ν density estimation
- Noise covariance Σ low-signal data regions
- Regularization parameters   Bayesian perspective...

  - Assume prior $h_l(\cdot) + b_l \sim \mathcal{GP}(0(\cdot), k(\cdot, \cdot)), l \in \{1, \ldots, L\}$
  - Include latent parameter variability ϵ_{x_l}
    in observed regressand model $x_l(\mathbf{q}) + b_l + \epsilon_{x_l}$

Model Selection

Online model selection: train *after* observing (unlabeled) test data

- Prior on known ν density estimation
- Noise covariance Σ low-signal data regions
- Regularization parameters   Bayesian perspective...

  - Assume prior $h_l(\cdot) + b_l \sim \mathcal{GP}(0(\cdot), k(\cdot, \cdot)), l \in \{1, \ldots, L\}$
  - Include latent parameter variability ϵ_{x_l}
    in observed regressand model $x_l(\mathbf{q}) + b_l + \epsilon_{x_l}$
  - If we further assume $\epsilon_{x_l} \sim \mathcal{N}(0, N\rho_l)$ then posterior mean
    function is KRR solution (12) [Rasmussen and Williams, 2005]
  - Reasonable to set $N\rho_l \leftarrow \text{cov}(x_l) \approx \frac{1}{N}\mathbf{x}_l^\mathsf{T}\mathbf{M}\mathbf{x}_l$

Model Selection

Online model selection: train *after* observing (unlabeled) test data

- Prior on known ν density estimation
- Noise covariance Σ low-signal data regions
- Regularization parameters $\rho_l \leftarrow \frac{1}{N^2}\mathbf{x}_l^\top \mathbf{M}\mathbf{x}_l$
  - Assume prior $h_l(\cdot) + b_l \sim \mathcal{GP}(0(\cdot), k(\cdot, \cdot)), l \in \{1, \ldots, L\}$
  - Include latent parameter variability ϵ_{x_l}
    in observed regressand model $x_l(\mathbf{q}) + b_l + \epsilon_{x_l}$
  - If we further assume $\epsilon_{x_l} \sim \mathcal{N}(0, N\rho_l)$ then posterior mean
    function is KRR solution (12) [Rasmussen and Williams, 2005]
  - Reasonable to set $N\rho_l \leftarrow \text{cov}(x_l) \approx \frac{1}{N}\mathbf{x}_l^\top \mathbf{M}\mathbf{x}_l$
- Kernel smoothing length-scale $\mathbf{\Lambda} \leftarrow \text{diag}\left(\sum_{n=1}^N \mathbf{q}_n\right)$

Model Selection

Online model selection: train *after* observing (unlabeled) test data

- Prior on known ν density estimation
- Noise covariance Σ low-signal data regions
- Regularization parameters $\rho_l \leftarrow \frac{1}{N^2} \mathbf{x}_l^\top \mathbf{M} \mathbf{x}_l$
  - Assume prior $h_l(\cdot) + b_l \sim \mathcal{GP}(0(\cdot), k(\cdot, \cdot)), l \in \{1, \ldots, L\}$
  - Include latent parameter variability ϵ_{x_l}
    in observed regressand model $x_l(\mathbf{q}) + b_l + \epsilon_{x_l}$
  - If we further assume $\epsilon_{x_l} \sim \mathcal{N}(0, N\rho_l)$ then posterior mean
    function is KRR solution (12) [Rasmussen and Williams, 2005]
  - Reasonable to set $N\rho_l \leftarrow \text{cov}(x_l) \approx \frac{1}{N} \mathbf{x}_l^\top \mathbf{M} \mathbf{x}_l$
- Kernel smoothing length-scale $\mathbf{\Lambda} \leftarrow \text{diag}\left(\sum_{n=1}^N \mathbf{q}_n \right)$

Some parameters still require manual selection...

- Prior on **x**   from tissue properties

Contribution

- Fast KRR method for nonlinear MRI parameter estimation

Contribution

- Fast KRR method for nonlinear MRI parameter estimation
    - Key insight: even with complicated MR signal models, can simulate training points "for free"
    - Convert *nonlinear estimation* problem into *nonlinear regression* problem that we solve in closed-form with kernels

Contribution

- Fast KRR method for nonlinear MRI parameter estimation
  - Key insight: even with complicated MR signal models, can simulate training points "for free"
  - Convert *nonlinear estimation* problem into *nonlinear regression* problem that we solve in closed-form with kernels

Ongoing work

- Performance analysis: how should N scale with L, Q?

Contribution

- Fast KRR method for nonlinear MRI parameter estimation
  - Key insight: even with complicated MR signal models, can simulate training points "for free"
  - Convert *nonlinear estimation* problem into *nonlinear regression* problem that we solve in closed-form with kernels

Ongoing work

- Performance analysis: how should N scale with L, Q?
- Exploit partially linear structure to incorporate scale invariance

Contribution

- Fast KRR method for nonlinear MRI parameter estimation
  - Key insight: even with complicated MR signal models, can simulate training points "for free"
  - Convert *nonlinear estimation* problem into *nonlinear regression* problem that we solve in closed-form with kernels

Ongoing work

- Performance analysis: how should N scale with L, Q?

- Exploit partially linear structure to incorporate scale invariance

- Validation on a compelling problem...

Advances in Quantitative MRI:

- **Acquisition**   [Ch. 4]
  How can we assemble fast, informative collections of scans
  to enable precise biomarker quantification?

- **Estimation**   [Ch. 5]
  Given data from an informative acquisition,
  how can we rapidly and accurately quantify these biomarkers?

- **Application**   [Ch. 6]
  Using these tools, can we design a state-of-the-art biomarker?

```
../fig/c,mwf/myelin.ps
```

www.mayoclinic.org

Myelin water fraction (MWF):

- Proportion of MR signal arising
from water trapped within healthy
myelin bilayers, relative to total
[Mackay et al., 1994]

../fig/c,mwf/myelin.ps

www.mayoclinic.org

Myelin water fraction (MWF):

- Proportion of MR signal arising
  from water trapped within healthy
  myelin bilayers, relative to total
  [Mackay et al., 1994]

- Correlates well with myelin content
  [Webb et al., 2003]

../fig/c,mwf/myelin.ps

www.mayoclinic.org

Multi-echo spin-echo (**MESE**)   [Mackay et al., 1994]

- Gold-standard
- Speed-limited by long repetition times ($\sim$2s)

Multi-echo spin-echo (**MESE**)   [Mackay et al., 1994]

- Gold-standard
- Speed-limited by long repetition times (∼2s)

Combinations of fast steady-state scans using variable flip angles ("**mcDESPOT**")   [Deoni et al., 2008]
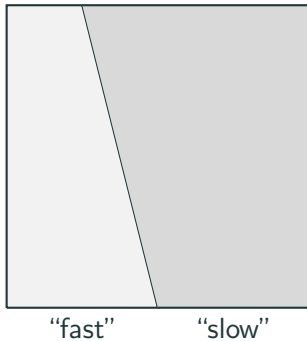
- Whole-brain, high-resolution MWF imaging in ∼30m
- Disagree with MESE MWF estimates,   [Zhang et al., 2015]
  likely due to insufficient precision   [Lankford and Does, 2013]

Multi-echo spin-echo (**MESE**)   [Mackay et al., 1994]

- Gold-standard
- Speed-limited by long repetition times ($\sim$2s)

Combinations of fast steady-state scans using variable flip angles ("**mcDESPOT**")   [Deoni et al., 2008]

- Whole-brain, high-resolution MWF imaging in $\sim$30m
- Disagree with MESE MWF estimates,   [Zhang et al., 2015] likely due to insufficient precision   [Lankford and Does, 2013]

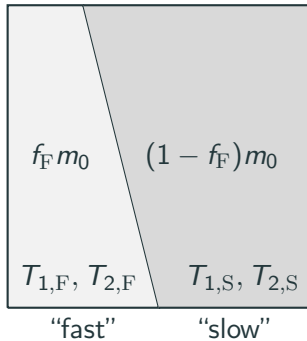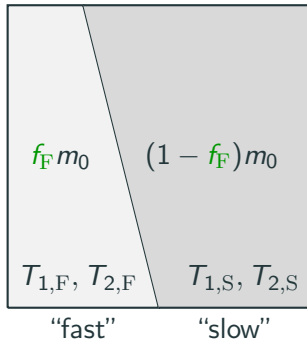**Goal**: fast, precise MWF quantification in WM

simple two-compartment model

"fast"   "slow"

simple two-compartment model

A voxel-scale MWF model

simple two-compartment model

Take fast-relaxing fraction f_{F} as a simple proxy for MWF

2-compartment SPGR model   [Spencer and Fishbein, 2000]

- included first-order physical exchange

2-compartment SPGR model   [Spencer and Fishbein, 2000]

- included first-order physical exchange
- neglected relaxation, precession, exchange during excitation

2-compartment SPGR model [Spencer and Fishbein, 2000]

- included first-order physical exchange

- neglected relaxation, precession, exchange during excitation

- absorbing off-resonance effects into m_0 *implies* neglecting exchange between excitation and readout

2-compartment SPGR model   [Spencer and Fishbein, 2000]

- included first-order physical exchange

- neglected relaxation, precession, exchange during excitation

- absorbing off-resonance effects into m_0 *implies* neglecting exchange between excitation and readout

Two-compartment DESS model   §6.2.2

- additional approximations required unless we assume time-independent diff in compartmental off-resonance freq

Multi-compartmental MR signal models

2-compartment SPGR model   [Spencer and Fishbein, 2000]

- included first-order physical exchange
- neglected relaxation, precession, exchange during excitation
- absorbing off-resonance effects into m_0 *implies* neglecting exchange between excitation and readout

Two-compartment DESS model   §6.2.2

- additional approximations required unless we assume time-independent diff in compartmental off-resonance freq
- including exchange, closed-form solutions still elusive

Multi-compartmental MR signal models

2-compartment SPGR model   [Spencer and Fishbein, 2000]

- included first-order physical exchange
- neglected relaxation, precession, exchange during excitation
- absorbing off-resonance effects into m_0 *implies* neglecting exchange between excitation and readout

Two-compartment DESS model   §6.2.2

- additional approximations required unless we assume time-independent diff in compartmental off-resonance freq
- including exchange, closed-form solutions still elusive

For simplicity, we neglect exchange.

$$\check{\mathbf{P}} \in \left\{ \arg \min_{\mathbf{P} \in \mathbb{P}} \bar{\Psi}(\mathbf{P}) \right\}, \text{ where}$$

$$\bar{\Psi}(\mathbf{P}) := \mathsf{E}_{\mathbf{x}, \boldsymbol{\nu}} \left(\text{tr} \left(\mathbf{W} \mathbf{F}^{-1}(\mathbf{x}; \boldsymbol{\nu}, \mathbf{P}) \mathbf{W}^{\mathsf{T}} \right) \right) \tag{15}$$

$$\check{\mathbf{P}} \in \left\{ \arg \min_{\mathbf{P} \in \mathbb{P}} \bar{\Psi}(\mathbf{P}) \right\}, \text{ where}$$

$$\bar{\Psi}(\mathbf{P}) := \mathsf{E}_{\mathbf{x}, \boldsymbol{\nu}} \left(\text{tr} \left(\mathbf{W} \mathbf{F}^{-1}(\mathbf{x}; \boldsymbol{\nu}, \mathbf{P}) \mathbf{W}^{\mathsf{T}} \right) \right) \quad (15)$$

- $\mathbf{x}$ $\qquad$ $[f_{\mathrm{F}}, T_{1,\mathrm{F}}, T_{2,\mathrm{F}}, T_{1,\mathrm{S}}, T_{2,\mathrm{S}}, m_0]^{\mathsf{T}}$
- $\boldsymbol{\nu}$ $\qquad$ flip angle variation
- $\mathbf{P}$ $\qquad$ SPGR/DESS nominal flip angles, repetition times

$$\check{\mathbf{P}} \in \left\{ \arg \min_{\mathbf{P} \in \mathbb{P}} \bar{\Psi}(\mathbf{P}) \right\}, \text{ where}$$

$$\bar{\Psi}(\mathbf{P}) := \mathsf{E}_{\mathbf{x},\nu}\left(\mathrm{tr}\left(\mathbf{W}\mathbf{F}^{-1}(\mathbf{x}; \nu, \mathbf{P})\mathbf{W}^{\mathsf{T}} \right) \right) \tag{15}$$

- $\mathbf{x}$ $[f_{\mathrm{F}}, T_{1,\mathrm{F}}, T_{2,\mathrm{F}}, T_{1,\mathrm{S}}, T_{2,\mathrm{S}}, m_0]^{\mathsf{T}}$
- ν flip angle variation
- $\mathbf{P}$ SPGR/DESS nominal flip angles, repetition times
- $\mathbf{W}$ $\mathsf{diag}\left(\left[(\mathsf{E}_{\mathbf{x},\nu}(f_{\mathrm{F}}))^{-1}, \mathbf{0}_5^{\mathsf{T}} \right]^{\mathsf{T}} \right)$

$$\check{\mathbf{P}} \in \left\{ \arg\min_{\mathbf{P}\in\mathbb{P}} \bar{\Psi}(\mathbf{P}) \right\}, \text{ where}$$

$$\bar{\Psi}(\mathbf{P}) := \mathsf{E}_{\mathbf{x},\boldsymbol{\nu}}\left(\mathrm{tr}\left(\mathbf{W}\mathbf{F}^{-1}(\mathbf{x};\boldsymbol{\nu},\mathbf{P})\mathbf{W}^{\mathsf{T}} \right) \right) \tag{15}$$

- $\mathbf{x}$ $[f_{\mathrm{F}}, T_{1,\mathrm{F}}, T_{2,\mathrm{F}}, T_{1,\mathrm{S}}, T_{2,\mathrm{S}}, m_0]^{\mathsf{T}}$
- ν flip angle variation
- $\mathbf{P}$ SPGR/DESS nominal flip angles, repetition times
- $\mathbf{W}$ $\mathrm{diag}\left(\left[(\mathsf{E}_{\mathbf{x},\boldsymbol{\nu}}(f_{\mathrm{F}}))^{-1}, \mathbf{0}_5^{\mathsf{T}} \right]^{\mathsf{T}} \right)$
- $\mathsf{E}_{\mathbf{x},\boldsymbol{\nu}}(\cdot)$ approximated via empirical averages
  of samples drawn from separable prior

Bayesian MWF Scan Design

$$\check{\mathbf{P}} \in \left\{ \arg \min_{\mathbf{P} \in \mathbb{P}} \bar{\Psi}(\mathbf{P}) \right\}, \text{ where}$$

$$\bar{\Psi}(\mathbf{P}) := \mathsf{E}_{\mathbf{x}, \nu}\left(\mathrm{tr}\left(\mathbf{W} \mathbf{F}^{-1}(\mathbf{x}; \nu, \mathbf{P}) \mathbf{W}^\mathsf{T} \right) \right) \qquad (15)$$

- $\mathbf{x}$ $[f_\mathrm{F}, T_{1,\mathrm{F}}, T_{2,\mathrm{F}}, T_{1,\mathrm{S}}, T_{2,\mathrm{S}}, m_0]^\mathsf{T}$
- ν flip angle variation
- $\mathbf{P}$ SPGR/DESS nominal flip angles, repetition times
- $\mathbf{W}$ $\mathrm{diag}\left(\left[(\mathsf{E}_{\mathbf{x}, \nu}(f_\mathrm{F}))^{-1}, \mathbf{0}_5^\mathsf{T} \right]^\mathsf{T} \right)$
- $\mathsf{E}_{\mathbf{x}, \nu}(\cdot)$ approximated via empirical averages
  of samples drawn from separable prior
- $\mathbb{P}$ nom flip angle, total scan time constraints

Optimized SPGR/DESS Acquisition

	Optimized flip angles (deg)	Optimized rep. times (ms)
SPGR	$38.1, 12.9, 9.2, 33.5$	$50.2, 32.4, 16.4, 11.8$
DESS	$32.0, 40.3, 52.9$	$17.5, 98.0, 37.6$

Table 3: Optimized Scan Parameters, $\check{\mathbf{P}}$

- Predicted MWF relative standard deviation in WM
  - Optimized SPGR/DESS: $\sqrt{\bar{\Psi}\left(\check{\mathbf{P}}\right)} = 0.285$
  - mcDESPOT: at least 1   [Lankford and Does, 2013]

Simulation Setup

- At each voxel, generate ground-truth $\mathbf{x}, \boldsymbol{\nu}$
- Using 2-compartment SPGR/DESS model $\mathbf{s}$ with optimized (and now fixed) parameters $\check{\mathbf{P}}$, generate voxel data $\mathbf{y} \in \mathbb{C}^{10}$

Simulation Setup

- At each voxel, generate ground-truth $\mathbf{x}, \nu$
- Using 2-compartment SPGR/DESS model $\mathbf{s}$ with optimized (and now fixed) parameters $\check{\mathbf{P}}$, generate voxel data $\mathbf{y} \in \mathbb{C}^{10}$

Use KRR to estimate just f_{F}

- Separable prior on $\mathbf{x}$: f_{F}, m_0 uniform; others log-uniform
- $N \leftarrow 10^6$ training points
- $Z \leftarrow 10^3$ kernel approximation order

MWF Estimation via KRR

Simulation Setup

- At each voxel, generate ground-truth $\mathbf{x}, \boldsymbol{\nu}$
- Using 2-compartment SPGR/DESS model $\mathbf{s}$ with optimized (and now fixed) parameters $\check{\mathbf{P}}$, generate voxel data $\mathbf{y} \in \mathbb{C}^{10}$

Use KRR to estimate just f_{F}

- Separable prior on $\mathbf{x}$: f_{F}, m_0 uniform; others log-uniform
- $N \leftarrow 10^6$ training points
- $Z \leftarrow 10^3$ kernel approximation order

Compare against grid search

- unconstrained search would require $\sim 100^5$ dictionary atoms
- we artificially constrain search here to limit computation

Fast-fraction f_{F} estimates, in simulation:

../fig/c,krr/sim.eps

Fast-fraction f_{F} estimates, in simulation:

../fig/c,krr/sim.eps

$\sim$4h   40s training, 2s testing

MWF Proof-of-concept Experimental Study

Acquired *in vivo* data using optimized MWF protocol

- Used $256 \times 256 \times 8$ 3D matrix over $24 \times 24 \times 4$cm FOV
- Required **11m48s** total (including BS scan)

MWF Proof-of-concept Experimental Study

Acquired *in vivo* data using optimized MWF protocol

- Used $256 \times 256 \times 8$ 3D matrix over $24 \times 24 \times 4$cm FOV
- Required **11m48s** total (including BS scan)

Rapidly estimated f_{F} as proxy for MWF

- Full-scale grid search intractable on typical desktop

MWF Proof-of-concept Experimental Study

Acquired *in vivo* data using optimized MWF protocol

- Used $256 \times 256 \times 8$ 3D matrix over $24 \times 24 \times 4$cm FOV
- Required **11m48s** total (including BS scan)

Rapidly estimated f_{F} as proxy for MWF

- Full-scale grid search intractable on typical desktop
- KRR training and testing took **35s** and **5s/slice**

MWF Proof-of-concept Experimental Study

Acquired *in vivo* data using optimized MWF protocol

- Used $256 \times 256 \times 8$ 3D matrix over $24 \times 24 \times 4$cm FOV
- Required **11m48s** total (including BS scan)

Rapidly estimated f_F as proxy for MWF

- Full-scale grid search intractable on typical desktop
- KRR training and testing took **35s** and **5s/slice**
- Iterative ML refinement took **29s/slice**

MWF Proof-of-concept Experimental Study

Acquired *in vivo* data using optimized MWF protocol

- Used $256 \times 256 \times 8$ 3D matrix over $24 \times 24 \times 4$cm FOV
- Required **11m48s** total (including BS scan)

Rapidly estimated f_F as proxy for MWF

- Full-scale grid search intractable on typical desktop
- KRR training and testing took **35s** and **5s/slice**
- Iterative ML refinement took **29s/slice**

Compared (qualitatively) with results in   [Zhang et al., 2015]

- GRASE: accelerated MESE acq   [Prasloski et al., 2012]
- mcDESPOT: 9 SPGR, 18 bSSFP scans   [Deoni, 2011]

../fig/c,mwf/ff,log2c-0,krr-ml.eps

../fig/c,mwf/mwf,gr/afieg/ep,mwf/mwf,mcdespot.eps

Contributions

- Two-compartment DESS signal model
- Fast acquisition for precise WM MWF estimation
- Proof-of-concept *in vivo* MWF images via KRR

Contributions

- Two-compartment DESS signal model
- Fast acquisition for precise WM MWF estimation
- Proof-of-concept *in vivo* MWF images via KRR

Ongoing work

- Systematic validation

Contributions

- Two-compartment DESS signal model
- Fast acquisition for precise WM MWF estimation
- Proof-of-concept *in vivo* MWF images via KRR

Ongoing work

- Systematic validation
- Further-optimized MWF acquisition

Table 4: Timeline to Defense

start date	task
2017-05	validate KRR estimation
2017-08	prepare KRR journal paper
2017-10	validate f_F estimates from SPGR/DESS acquisition
2018-01	prepare fast MWF imaging journal paper
2018-03	defend dissertation

Future Work

Table 4: Timeline to Defense

start date	task
2017-05	validate KRR estimation
2017-08	prepare KRR journal paper
2017-10	validate f_F estimates from SPGR/DESS acquisition
2018-01	prepare fast MWF imaging journal paper
2018-03	defend dissertation

Longer-term research directions

- combine image reconstruction and KRR estimation
- correlate our MWF estimates with other myelin biomarkers
- apply KRR to other problems

References i

Cramér, H. (1946).
Mathematical methods of statistics.
Princeton Univ. Press, Princeton.

Aronszajn, N. (1950).
Theory of reproducing kernels.
Trans. Amer. Math. Soc., 68(3):337–404.

Bertsimas, D. and Tsitsiklis, J. (1993).
Simulated annealing.
Statistical Science, 8(1):10–15.

Deoni, S. C. L. (2011).
**Correction of main and transmit magnetic field (B0 and B1)
inhomogeneity effects in multicomponent-driven equilibrium
single-pulse observation of T1 and T2.**
Mag. Res. Med., 65(4):1021–35.

Deoni, S. C. L., Rutt, B. K., Arun, T., Pierpaoli, C., and Jones, D. K. (2008).
Gleaning multicomponent T1 and T2 information from steady-state imaging data.
Mag. Res. Med., 60(6):1372–87.

Keenan, K. E., Stupic, K. F., Boss, M. A., Russek, S. E., Chenevert, T. L., Prasad, P. V., Reddick, W. E., Cecil, K. M., Zheng, J., Hu, P., and Jackson, E. F. (2016).
Multi-site, multi-vendor comparison of T1 measurement using ISMRM/NIST system phantom.
In *Proc. Intl. Soc. Mag. Res. Med.*, page 3290.

Lankford, C. L. and Does, M. D. (2013).
On the inherent precision of mcDESPOT.
Mag. Res. Med., 69(1):127–36.

Mackay, A., Whittall, K., Adler, J., Li, D., Paty, D., and Graeb, D. (1994).
In vivo visualization of myelin water in brain by magnetic resonance.
Mag. Res. Med., 31(6):673–7.

Nataraj, G., Nielsen, J.-F., and Fessler, J. A. (2017).
Optimizing MR scan design for model-based T1, T2 estimation from steady-state sequences.
IEEE Trans. Med. Imag., 36(2):467–77.

Prasloski, T., Rauscher, A., MacKay, A. L., Hodgson, M., Vavasour, I. M., Laule, C., and Mädler, B. (2012).
Rapid whole cerebrum myelin water imaging using a 3D GRASE sequence.
NeuroImage, 63(1):533–9.

References iv

Rahimi, A. and Recht, B. (2007).
Random features for large-scale kernel machines.
In *NIPS*.

Rasmussen, C. E. and Williams, C. K. I. (2005).
Gaussian processes for machine learning (adaptive computation and machine learning).
MIT Press.

Redpath, T. W. and Jones, R. A. (1988).
FADE-A new fast imaging sequence.
Mag. Res. Med., 6(2):224–34.

Schölkopf, B., Herbrich, R., and Smola, A. J. (2001).
A generalized representer theorem.
In *Proc. Computational Learning Theory (COLT)*, pages 416–426.
LNCS 2111.

References v

Spencer, R. G. and Fishbein, K. W. (2000).
Measurement of spin-lattice relaxation times and concentrations in systems with chemical exchange using the one-pulse sequence: breakdown of the Ernst model for partial saturation in nuclear magnetic resonance spectroscopy.
J. Mag. Res., 142(1):120–35.

Webb, S., Munro, C. A., Midha, R., and Stanisz, G. J. (2003).
Is multicomponent T2 a good measure of myelin content in peripheral nerve?
Mag. Res. Med., 49(4):628–45.

Zhang, J., Kolind, S. H., Laule, C., and MacKay, A. L. (2015).
Comparison of myelin water fraction from multiecho T2 decay curve and steady-state methods.
Mag. Res. Med., 73(1):223–32.

Zur, Y., Wood, M. L., and Neuringer, L. J. (1991).
Spoiling of transverse magnetization in steady-state sequences.
Mag. Res. Med., 21(2):251–63.